PRESSURE AND PRESSURE DERIVATIVE TYPE CURVES OF A VERTICAL WELL COMPLETED WITHIN A PAIR OF INCLINED SEALING FAULTS

BY

EZIUZOR DANIEL TOBECHUKWU

ENG1604321

DEPARTMENT OF PETROLEUM ENGINEERING

FACULTY OF ENGINEERING

UNIVERSITY OF BENIN

BENIN CITY

DECEMBER, 2022

PRESSURE AND PRESSURE DERIVATIVE TYPE CURVES OF A VERTICAL WELL COMPLETED WITHIN A PAIR OF INCLINED SEALING FAULTS

BY

EZIUZOR DANIEL TOBECHUKWU

ENG1604321

A PROJECT SUBMITTED TO THE DEPARTMENT OF PETROLEUM ENGINEERING, FACULTY OF ENGINEERING, UNIVERSITY OF BENIN, BENIN CITY

IN PARTIAL FULFILLMENT OF THE REQUIREMENTS FOR THE AWARD OF BACHELOR DEGREE IN PETROLEUM ENGINEERING

DECEMEBER, 2022

CERTIFICATION

This is to certify that this research project was carried out by EZIUZOR DANIEL TOBECHUKWU of the Department of Petroleum Engineering at the University of Benin, Benin City, Edo State, Nigeria, under the supervision of Professor E.S Adewole.

…… …..…….

Professor E.S. Adewole Date

Project Supervisor

……

Dr. Taiwo Seun …..…….

Project Coordinator Date

……

Dr. Ikponmwosa Ohenhen …..…….

Head of Department Date

…… …..…….

Prof. S. O. Isehunwa Date

External Supervisor

DEDICATION

This project is dedicated to Almighty God for His infinite mercy in seeing me through the project, my supervisor for its impact and perseverance, and to my family for their morale and financial support throughout my stay in the University of Benin, department of petroleum engineering

ACKNOWLEDGEMENT

I wish to express my appreciation of the efforts of my parents Mr AND Mrs EZIUZOR and my siblings for their moral and financial assistance, my supervisor, Professor E.S. Adewole for his invaluable support and guidance towards the completion of this project, the Head of Department, Dr. Ikponmwosa Ohenhen, and the entire lecturers and staff of the Department of Petroleum Engineering, University of Benin for their knowledge and impacts to my success thus far, my course mates who has supported in one way or the other, to my extended family for their support and selfless services towards my success, may GOD sufficiently bless you all.

ABSTRACT

Type curves come in handy when our pressure buildup and pressure drawdown analysis do not yield a straight line hence generating a master curve for wells completed within a pair of sealing faults. The type curves from an observed data is superimposed on the master curve to estimate reservoir system properties. A sealing fault creates image wells, which communicate with each other and the object well. As a result, object well performance can be affected by reservoir boundaries, and positioning of a well therefore must be strategic to ensure oil production for a long time. This is because pressure drop across the producing well is the addition of the pressure drop of the object well and the several image wells created because of the inclination. This is the principle of superposition. The inclination of a sealing fault influences the number of image wells, n, with the model $n = (360/\theta) - 1$. With different angles of inclination of the sealing faults, polygons are constructed to determine the distances between the object well and corresponding image wells.

In this paper, both dimensionless pressure and dimensionless pressure derivatives type curves as functions of number of image wells, are produced assuming that a vertical well is completed within a pair sealing faults. Wellbore storage and skin effects are considered. The results provide distances for several angles of inclination. Object well design, image well distances and faults angle affect dimensionless pressure and dimensionless pressure derivative. Dimensionless pressure and dimensionless pressure derivative of $1.1513(n+1)$ per cycle and $0.5(n+1)$, respectively are observed.

Generating dimensionless pressure derivative curves helps the engineer to identify the point where the hump expires and where the straight-line analysis begins. That is the right point for well test analysis.

Table of Contents

LIST OF TABLES

LIST OF FIGURES

NOMENCLATURE

θ = Angle of inclination between intersecting faults, degrees (^{o})

n = number of images

P_D = dimensionless pressure

t_D = dimensionless time

d = Distance between well and inclined faults, ft

Cd = dimensionless wellbore storage coefficient

Ow = Object well

CHAPTER ONE

INTRODUCTION

1.1 Background of study

Type curve analysis is a method for quantifying well and reservoir parameters such as permeability, skin, fracture half-length, dual-porosity parameters, and others, by comparing the pressure change and its derivative of the acquired data to reservoir model curve families, called type curves. When a match is found between data and a type curve, the parameters that characterize the behaviour of the model providing a match are thereby determined (Earlougher, R.C. Jr. (1977), Matthews, C.S et al (1967)). Originally, type-curve analysis was done manually using only the pressure change. With the introduction of the pressure derivative, the analysis requires matching both pressure change and its derivative. Computer-assisted matching permits rigorous accounting for superposition in time due to flow-rate variations before and even during (in the case of drawdown analysis) the transient data acquisition, as well as providing a continuum of solutions instead of a type-curve family derived from discrete values for the governing parameters. Type curve are families of the paired pressure change and its derivative computed from a model. The model is usually generated from an analytical solution of the diffusion equation with boundary conditions strategically defined to enable observation of theoretical trends in the pressure-transient response. The boundary conditions that can be defined near the well include constant or variable wellbore storage, limited entry (partial penetration), radial composite (damage skin due to permeability alteration), and a fracture extending the cylindrical wellbore to an extended plane. The borehole trajectory can be vertical, angled, or horizontal. The distant boundary conditions include a sealing or partially sealing planar boundary (fault), intersecting faults and rectangular boundaries (sealing or constant pressure) (Overpeck, A.C et al, (1970), Prasad, Raj K., (1975)).

Furthermore, the diffusion equation can be adjusted to accommodate reservoir heterogeneity in the form of dual porosity or layering. Finally, when generated with computer assistance, the type-curve family can account for superposition in time due to flow-rate variations before and even during the transient data acquisition. Originally, type-curve families were printed on specialized (usually log-log) coordinates with dimensionless parameters defining the x and y axes. Today, commercial software can generate the type-curve families on the computer screen, enabling a much more flexible and user-friendly analysis. Further, automated regression (usually least squares) permits an optimized match between the acquired data and a selected model. Type curves have greatly enriched the ability of interpreters to extract potential explanations for transient data trends that differ from the radial-flow behaviour required for conventional semilog analysis (Britton, P.R. et al (1988), Adewole, E.S. (2021)).

Type curves provide a powerful method for analysing pressure drawdown (flow) and build-up tests. Fundamentally, type curves are pre-plotted solutions to the flow equations, such as the diffusivity equation, for selected types of formations and selected initial and boundary conditions. Because of the way they are plotted (usually on logarithmic coordinates), it is convenient to compare actual field data plotted on the same coordinates to the type curves. The results of this comparison frequently include qualitative and quantitative descriptions of the formation and completion properties of the tested well (Prasad, R. K., (1975), Tiab, D. and Kumar, A. (1980)).

1.2 Statement of problem

1. Obtain distances between object wells and image wells from the sealing faults
2. The distances are a major attribute of the Pd and Pd' model used to generate this master-curve.

3. Determination of well placement for optimum oil and gas production that is as far as possible away from the sealing faults.

1.3 Aims and Objectives:

1. To construct curves Pd and Pd' for a vertical well completed within a pair of inclined sealing faults.
2. To investigate effects of faults inclination, number of images, well design and image distances on wellbore pressure distribution**.**
3. To provide a guide for well useful location options.
4. Investigate conditions that can prolong oil production from wells within a pair of sealing faults.

1.4 Scope of Study

The scope of this study is simply to generate a master curve which can be superimposed by the conventional test curve. The distance of the well from the boundary is our thesis in this work, being able to place a place farther from the boundary (two inclined sealing faults) is of our outermost concern. The sealing faults therefore act as plane mirror to the object well thereby creating other image wells.

1.5 Relevance of Study

Type curves are pre-plotted solutions of our diffusivity equation. When our conventional test analysis do not yield a straight line for solution, type curves help them come in handy to help characterize the reservoir obtaining properties such as permeability, skin factor, transmissibility etc.

CHAPTER TWO

LITERATURE REVIEW

2.1 Type curves

The type curve analysis approach was introduced in the petroleum industry by Agarwal et al. (1970) as a valuable tool when used in conjunction with conventional semilog plots. A type curve is a graphical representation of the theoretical solutions to flow equations. The type curve analysis consists of finding the theoretical type curve that "matches" the actual response from a test well and the reservoir when subjected to changes in production rates or pressures. The match can be found graphically by physically superposing a graph of actual test data with a similar graph of type curve(s) and searching for the type curve that provides the best match. Since type curves are plots of theoretical solutions to transient and pseudo-steady-state flow equations, they are usually presented in terms of dimensionless variables (e.g., pD, tD, rD, and CD) rather than real variables (e.g., Δp, t, r, and C). The reservoir and well parameters, such as permeability and skin, can then be calculated from the dimensionless parameters defining that type curve. Any variable can be made "dimensionless" by multiplying it by a group of constants with opposite dimensions, but the choice of this group will depend on the type of problem to be solved. For example, to create the dimensionless pressure drop pD, the actual pressure drop Δp in psi is multiplied by the group A with units of psi−1, or: pD = AΔp Finding the group A that makes a variable dimensionless is derived from equations that describe reservoir fluid flow.

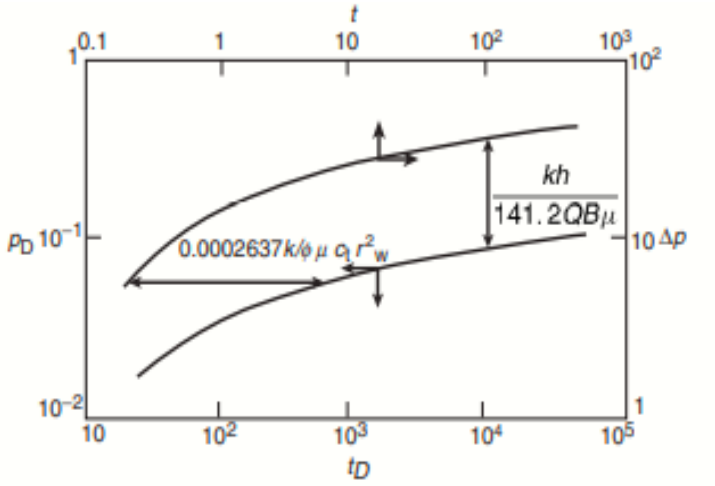

Figure 2.1.1: Concept of Type curves.

2.2 Type curves used to interpret vertical well test

Type curves first appeared in oil industry sure in the seventies. Several kinds, as listed below, are used to interpret a test in a vertical well with an infinite homogeneous reservoir

Agarwa et al type

Curver Moonley type curve

Earlougher and Kersch type curves

Gringarten et al type curves

2.3 Advantages and limitations of type curves well models:

Type curves help the interpreter to:

1. Make a diagnosis about the type of reservoir and understand the flow use conventional methods by determining the sequence of flow regimes
2. In a homogeneous reservoir type curves can be used to locate the end of the wellbore storage effect and thereby situate the semi-log straight line correctly.

The type curve representation has two important limitations in an infinite homogeneous reservoir:

1. The wellbore storage effect is represented by a constant value
2. A test needs to be interpreted with type curves established for drawdown.

The second limitation can be eliminated if the interpreter uses a well model instead of a set of type curves. A well model is an analytic program used to generate type curves taking then flow rate history into account.

Additionally, the representation by a set of curves severely limits the number of parameters that can be taken into account.

It was possible to establish a set of type curves to interpret a test for an infinite homogeneous reservoir since only three parameters govern the pressure variations: wellbore storage, permeability and skin.

When the reservoir-well configuration is more complex, the number of parameters becomes too large for a type curve representation. A well model is the only way to generate appropriate type curves.

Type curves represented in sets or generated by a well model undergo the same flattening out effect due to the logarithmic representation.

The scale attenuates pressure variations. Because of this interpreting with type curves is often tricky. For a long time the problem discouraged interpreters who were used to the sensitivity of conventional methods.

2.4 Dimensionless Pressure Derivative

The preceding chapter showed the advantages and drawbacks of type curves: advantages related to the fact that one single curve can deal with a whole test and drawbacks related to the log-log representation that makes it difficult to observe small relative pressure variations.

Methods using the pressure derivative take advantage of the advantages of the type curve representation and counteract the drawbacks of the logarithmnic representation.

These methods are based on an observed fact: in a well test the pressure variation is more significant than the pressure itself. This is illustrated by the fact that it is the slope of the semi-log straight lines that is used to get information on the reservoir in conventional methods.Like type curves, the derivative offers the great advantage of allowing a complete well test to be taken into account and Interpreted using one single curve.Each type of flow exhibits a characteristic facies on the derivative which represents an excellent diagnostic tool. By materializing pressure variations the derivative is similar to a zoom onto the data, amplifying variations that would otherwise not be noticed flattened out by the logarithmic representation.

The following chapters illustrate the contribution of the derivative in more complex reservoir-well configurations.

Smoothing algorithms are required to overcome the main limitation on its use due to the noise of the signal. The derivative is practically impossible to calculate by hand: a computer is necessary. It has become one of the major tools in well test analysis software.

CHAPTER THREE

METHODOLOGY

3.1 Methodology

Wells communicate with each other and as a result can be affected by their surroundings, positioning of a well must be strategic so as to ensure oil production for a long time. We would have to inspect the boundary conditions, in this case is a pair of inclined sealed faults. A well between two sealing faults provides images corresponding to the angle of inclination, the larger the angle if inclination, the smaller the number of images produced; images are produced until they converge at a point forming polygons.

A proposed model relating the number of images to the angle of inclination is: $n= \frac{360}{\theta} - 1$,

where n is the number of images and θ is the angle of inclination. Well images must therefore be considered as pressure drop across wells becomes addition of the pressure drop of the object well and the image wells. Calculation of slope is given the formula 1.1513 + 1.1513n = m, where m is slope and n is the number of image wells.

Dimensionless pressure across a well inclined at an angle is given as

$$Pd = -0.5Ei\left(\frac{-r2}{4td}\right) + s - 0.5\sum Ei\left(\frac{d}{4^n}\frac{1}{td^n}\right) \quad \text{(1)}$$

Where $Ei\left(\frac{d}{4^n}\frac{1}{td^n}\right) = Ei\left(\frac{d1^2 d2^2 d3^2 \ldots dn^2}{4^n td^n}\right)$

While the dimensionless pressure derivative is given as

$$P'_d = 0.5\left(\exp\left(\frac{-r2}{4t_d}\right) + \exp\left(\left(\frac{d}{4^n}\frac{1}{td^n}\right)\right)\right. \quad \text{(2)}$$

Figure 3.1.1 shows a well completed within two sealing faults inclined

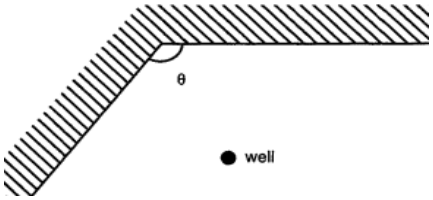

Figure 3.1.1: A Vertical Well Completed within Two Inclined Sealing Faults at angle θ.

The number of images n, formed is related with the angle of inclination as follows:

$$n = \frac{360}{\theta} - 1 \qquad (3)$$

During infinite-acting flow, the horizontal well experiences infinite plane (y and z axes), and slab (x axis) sources in an infinite slab reservoir. Hence, its dimensionless pressure drop is derived during this period as follows (Tiab, D. et al, (1980), Earlougher, R.C. Jr. (1977)):

$$p_D = -\frac{1}{2}\mathrm{Ei}\left[-\frac{r_D^2}{4t_D}\right] + s \qquad (4)$$

Following Equation. 1, the dimensionless pressure derivative is

$$p_D' = \frac{1}{2}\exp\left[-\frac{r_D^2}{4t_D}\right] \qquad (5)$$

A well between two sealing faults produces images corresponding to the angle of inclination. The larger the angle of inclination, the smaller the number of images produced according to Equation 1. The images can be located either by use of an appropriate software or analytically by trigonometry or by drawing perpendicular rays from one image through a polygon of side (n+1). Where the intersecting ray meets a mirror is an image. Since pressure drop in the object is affected by pressure drops in the image wells, by superposition principle, pressure drop in the object well becomes addition of the pressure drop of the object well and the image wells. In dimensionless pressure form, the total pressure drop in the object well within a pair of faults inclined at an angle is given as:

$$p_D = -\frac{1}{2}\left[Ei\left(-\frac{1}{4\,t_D/c_D}\right)+s+Ei\left(-\frac{d_{1D}^2}{4t_D}\right)+Ei\left(-\frac{d_{2D}^2}{4t_D}\right)+Ei\left(-\frac{d_{3D}^2}{4t_D}\right)+\ldots\ldots..+Ei\left(-\frac{d_{Dn}^2}{4t_D}\right)\right] \quad (6)$$

The corresponding dimensionless pressure derivative will be:

$$p_D' = \frac{1}{2}\left[\exp\left(-\frac{1}{4\,t_D/c_D}\right)+\exp\left(-\frac{d_{1D}^2}{4t_D}\right)+\exp\left(-\frac{d_{2D}^2}{4t_D}\right)+\exp\left(-\frac{d_{3D}^2}{4t_D}\right)+\ldots\ldots..+\exp\left(-\frac{d_{Dn}^2}{4t_D}\right)\right] \quad (7)$$

Where d_1, d_2, d_3 …dn are image well distances from the object well.

Equations 4 and 5 are solved for different sealing faults angles, same object well design and object distances from the faults. Results are plotted on same axes as type curves for ideal, damaged, and stimulated object wellbore. Wellbore storage is also varied. Throughout the computation, D = 44.2815ft.

CHAPTER FOUR

RESULTS AND DISCUSSION

4.1 Polygons formed due to inclination of sealing fault

A fault inclined at 45 degrees would result in 8 number of images wells, and therefore the shortest distance between these image wells and the object well would need to be determined to know the influence each image well as on the object well.

A generalized formula of the shortest image to object well distance is generated for each polygon assuming an equal distance "d" from the two inclined sealing faults acting as mirrors. This equal distance has therefore enable a convergence of different regular polygons depending on the angle of inclination. Where Ow symbolizes Object well, W1 is image well one, W2= image well two, D1 is the shortest distance from image well one to object well, likewise for D2, D3 etc.

Octagon: a regular octagon as an interior angle of 135 degrees, A regular octagon has a seven well images with shortest distance from Image well one (W1) to the Object well (Ow) as 2d. The following are the shortest distances from each image well to the object well.

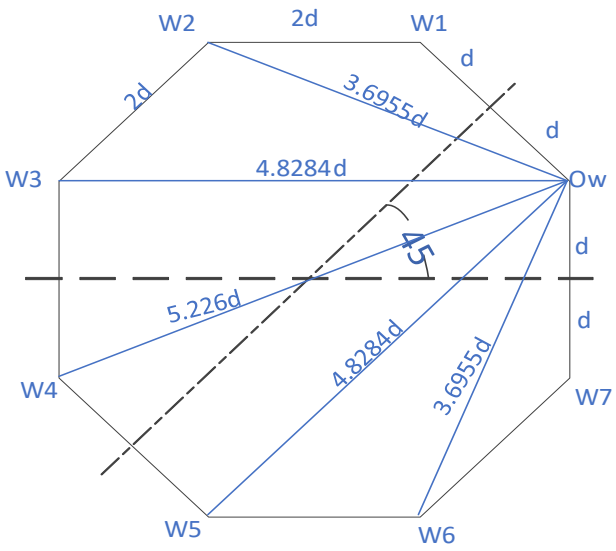

Figure 4.1.1: Sealing fault inclined at angle 45

4.1.1 Analysis of generalized distance for a regular octagon

$\frac{sin135}{X}=\frac{sin22.5}{2d}$

$\frac{2dsin135}{sin22.5}$=3.6955d

Since angle in an interior octagon is 135,

135-22.5=112.5

2d and 3.6955d (an angle between known sides)

Using cosine rule:

$D_3=\sqrt{(2d^2)^2+(3.6955D)^2}-2(2D)*3.6955cos112.5$

$4D^2$+13.6567d^2+5.6568d^2=$\sqrt{23.3135d^2}$

D_3=4.8284d

$D_4=\sqrt{(2d)^2}$+ (4.8284d)^2-2(2d*4.8284d*cos90)

=$\sqrt{4d^2}$+23.3134D^2

=5.2262268d=D_4

$D_5 = D_3 = 4.8284d$ (Similar triangles)

$D_6 = D_2 = 3.6955d$ (Similar triangles)

D1=2d

D2=3.6599d

D3=4.8284d

D4=5.226d

D5=4.8284d

D6=3.6599d

D7=2d

$$Pd = -0.5(EI(\frac{-r2}{4t_d}) + EI(\frac{D1^2}{4t_d}) + EI(\frac{D2^2}{4t_d}) + EI(\frac{D3^2}{4t_d}) + EI(\frac{D4^2}{4t_d}) + EI(\frac{D5^2}{4t_d}) + EI(\frac{D6^2}{4t_d}) + EI(\frac{D7^2}{4t_d})) \quad (8)$$

$$P'd = 0.5(\exp(\frac{-r2}{4t_d}) + \exp(\frac{D1^2}{4t_d}) + \exp(\frac{D2^2}{4t_d}) + \exp(\frac{D3^2}{4t_d}) + \exp(\frac{D4^2}{4t_d}) + \exp(\frac{D5^2}{4t_d}) + \exp(\frac{D6^2}{4t_d}) + \exp(\frac{D7^2}{4t_d})) \quad (9)$$

After generating the type curve is was calculated that the number of images n, to be 6.99

Hexagon: A regular hexagon has an interior angle of 120 degrees, five well images with shortest distance from each Image well to the Object well (Ow). The following are the shortest distances from each image well to the object well.

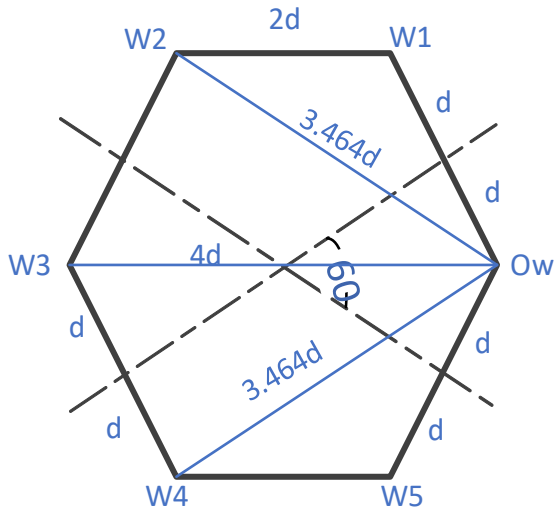

Figure 4.1.2: Sealing fault inclined at angle 60

4.1.2 Analysis of generalized distance for a regular hexagon

$$\frac{sin120}{X} = \frac{sin30}{2d}$$

$X=\frac{sin120*2d}{sin30}$

$D2=2\sqrt{3d}$

$D_4 = D_2 = 2\sqrt{3}$d (similar triangle)

$D_5 = 2d$

$$\frac{sin90}{X} = \frac{sin30}{20}$$

$$\frac{2d}{sin30} = 4d = D_3$$

D1=2d

D2=3.464d

D3=4d

D4=3.464d

D5=2d

$$Pd = -0.5(EI\ (\frac{-r2}{4t_d}) + EI\ (\frac{D1^2}{4t_d}) + EI\ (\frac{D2^2}{4t_d}) + EI\ (\frac{D3^2}{4t_d}) + EI\ (\frac{D4^2}{4t_d}) + EI\ (\frac{D5^2}{4t_d}) \quad (10)$$

$$P'_d = 0.5(\exp\ (\frac{-r2}{4t_d}) + \exp\ (\frac{D1^2}{4t_d}) + \exp\ (\frac{D2^2}{4t_d}) + \exp\ (\frac{D3^2}{4t_d}) + \exp\ (\frac{D4^2}{4t_d}) + \exp\ (\frac{D5^2}{4t_d})) \quad (11)$$

After generating the type curve is was calculated that the number of images n, to be 4.99

Pentagon: A regular Pentagon has an interior angle of 108 degrees and four well images. The following are the shortest distances from each image well to the object well.

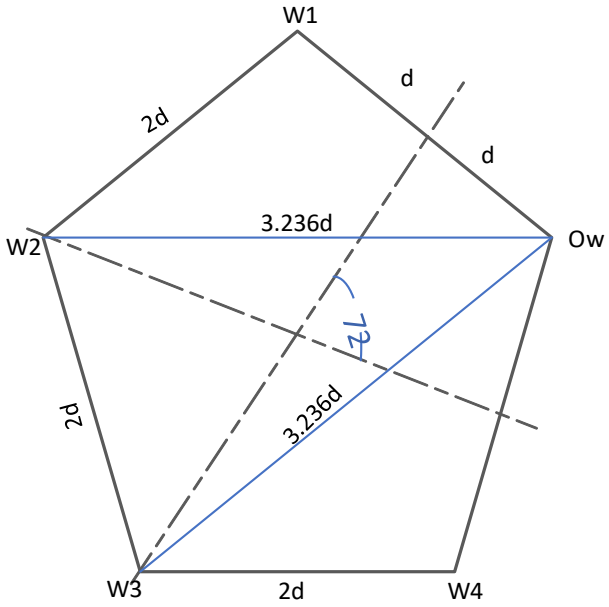

Figure 4.1.3: Sealing fault inclined at angle 72

4.1.3 Analysis of generalized distance for a pentagon

$$\frac{sin108}{X} = \frac{sin36}{2d}$$

D_2=X=3.236 d

$(2d)^2 + 2d^2$

to find D3, consider similar triangles

D_3=$\frac{sin108}{x} = \frac{sin36}{2d}$

Where D3= 3.236d=D2

D1=2d

D2=3.236d

D3=3.236d

D4=2d

$$Pd = -0.5(EI\left(\frac{-r2}{4t_d}\right) + EI\left(\frac{D1^2}{4t_d}\right) + EI\left(\frac{D2^2}{4t_d}\right) + EI\left(\frac{D3^2}{4t_d}\right) + EI\left(\frac{D4^2}{4t_d}\right)) \quad (12)$$

$$P'_d = 0.5(\exp\left(\frac{-r2}{4t_d}\right) + \exp\left(\frac{D1^2}{4t_d}\right) + \exp\left(\frac{D2^2}{4t_d}\right) + \exp\left(\frac{D3^2}{4t_d}\right) + \exp\left(\frac{D4^2}{4t_d}\right)) \quad (13)$$

After generating the type curve is was calculated that the number of images n, to be 3.99

Quadrilateral: A Square has an interior angle of 90 degrees, three well images with shortest distance from Image well one (W1) to the Object well (Ow) as '2d'. The following are the shortest distances from each image well to the object well.

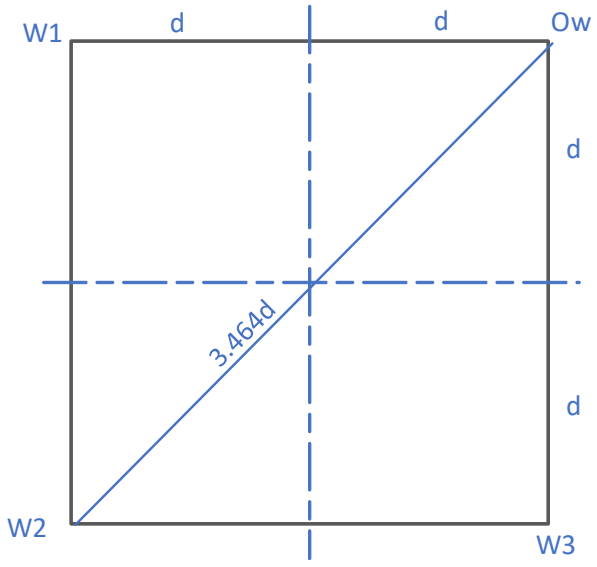

Figure 4.1.4: Sealing fault inclined at angle 90

4.1.4 Analysis of generalized distance for a Quadrilateral

$D_2 = \sqrt{(2d^2 + (2d)^2}$

$= 4d^2 + 4d^2$

D_2=$\sqrt{8d^2} = 2\sqrt{3}d$=3.464d

D1=2d

D2=$2\sqrt{3}d$ = 3.464d

D3=2d

$$Pd = -0.5(EI\left(\frac{-r2}{4t_d}\right) + EI\left(\frac{D1^2}{4t_d}\right) + EI\left(\frac{D2^2}{4t_d}\right) + EI\left(\frac{D3^2}{4t_d}\right)) \quad (14)$$

$$P'_d = 0.5(\exp\left(\frac{-r2}{4t_d}\right) + \exp\left(\frac{D1^2}{4t_d}\right) + \exp\left(\frac{D2^2}{4t_d}\right) + \exp\left(\frac{D3^2}{4t_d}\right)) \quad (15)$$

After generating the type curve is was calculated that the number of images n, to be 2.99

Triangle: Seeing we would have a regular triangle; it would then mean that this is an equilateral triangle having all sides equal with an interior angle of 60 degrees each. Well images produced here are just two following our model.

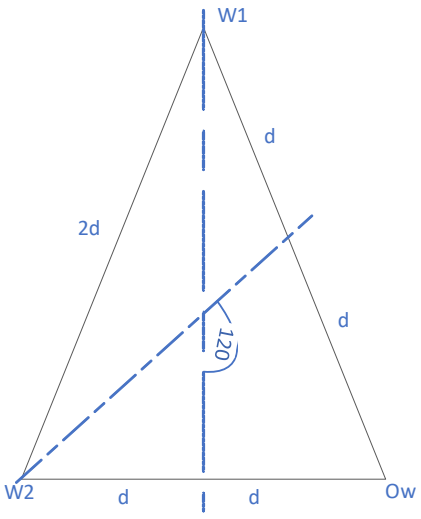

Figure 4.1.5: Sealing fault inclined at angle 120

D1= 2d

D2=2d

$$Pd = -0.5(EI\left(\frac{-r2}{4t_d}\right) + EI\left(\frac{D1^2}{4t_d}\right) + EI\left(\frac{D2^2}{4t_d}\right)) \quad (16)$$

$$P'_d = 0.5(\exp\left(\frac{-r2}{4t_d}\right) + \exp\left(\frac{D1^2}{4t_d}\right) + \exp\left(\frac{D2^2}{4t_d}\right)) \quad (17)$$

After generating the type curve is was calculated that the number of images n, to be 1.99

Table 4.1.1: Table of results for regular polygons

Θ (angles of inclination)	Number of image wells	Polygons formed
45	6.99	Octagon
60	4.99	Hexagon
72	3.99	Pentagon
90	2.99	Quadrilateral
120	1.99	Triangle

4.2 Type curves of well inclined at an angle of unequal distances

A well in between two inclined sealing faults of unequal distances yields and irregular polygon with the model.

4.2.1 Procedure of constructing irregular octagon

1. Construct a regular decagon first
2. Join two points on the decagon say in this case, point Ow to W7
3. Do likewise for point W3 to W4

$$Pd = -0.5(EI\left(\frac{-r2}{4t_d}\right) + EI\left(\frac{D1^2}{4t_d}\right) + EI\left(\frac{D2^2}{4t_d}\right) + EI\left(\frac{D3^2}{4t_d}\right) + EI\left(\frac{D4^2}{4t_d}\right) + EI\left(\frac{D5^2}{4t_d}\right) + EI\left(\frac{D6^2}{4t_d}\right) + EI\left(\frac{D7^2}{4t_d}\right)) \quad (18)$$

$$P'_d = 0.5(\exp\left(\frac{-r2}{4t_d}\right) + \exp\left(\frac{D1^2}{4t_d}\right) + \exp\left(\frac{D2^2}{4t_d}\right) + \exp\left(\frac{D3^2}{4t_d}\right) + \exp\left(\frac{D4^2}{4t_d}\right) + \exp\left(\frac{D5^2}{4t_d}\right) + \exp\left(\frac{D6^2}{4t_d}\right) + \exp\left(\frac{D7^2}{4t_d}\right)) \quad (19)$$

Applying our Pd and P'd formula gives us a result similar to that of a regular octagon yielding number of images to be 6.99

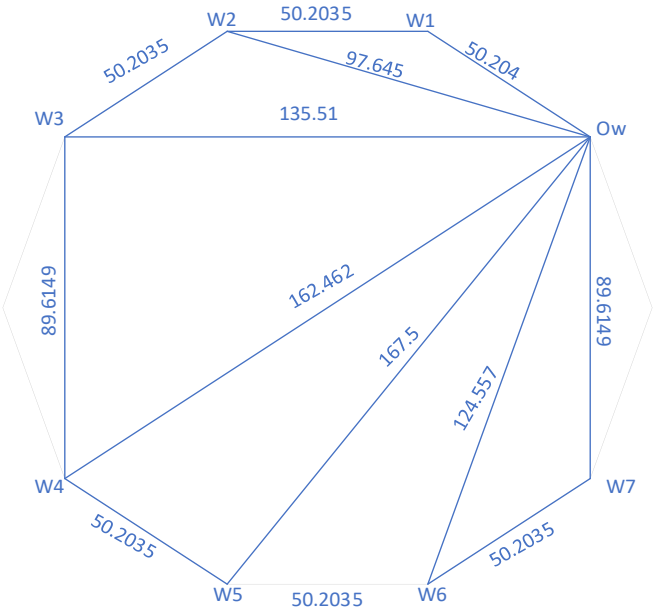

Figure 4.2.1: Inclination of sealing fault at angle 45 at unequal distances from the object well

4.2.2 Procedure of constructing an irregular hexagon

1. Construct a regular decagon first.
2. Join two points on the decagon say in this case, point Ow to W7
3. Do likewise for point W3 to W4

$$Pd = -0.5(EI\left(\frac{-r2}{4t_d}\right) + EI\left(\frac{D1^2}{4t_d}\right) + EI\left(\frac{D2^2}{4t_d}\right) + EI\left(\frac{D3^2}{4t_d}\right) + EI\left(\frac{D4^2}{4t_d}\right) + EI\left(\frac{D5^2}{4t_d}\right)) \quad (20)$$

$$P'_d = 0.5(\exp\left(\frac{-r2}{4t_d}\right) + \exp\left(\frac{D1^2}{4t_d}\right) + \exp\left(\frac{D2^2}{4t_d}\right) + \exp\left(\frac{D3^2}{4t_d}\right) + \exp\left(\frac{D4^2}{4t_d}\right) + \exp\left(\frac{D5^2}{4t_d}\right)) \quad (21)$$

Applying our Pd and P'd formula gives us a result similar to that of a regular hexagon yielding number of images to be 4.99

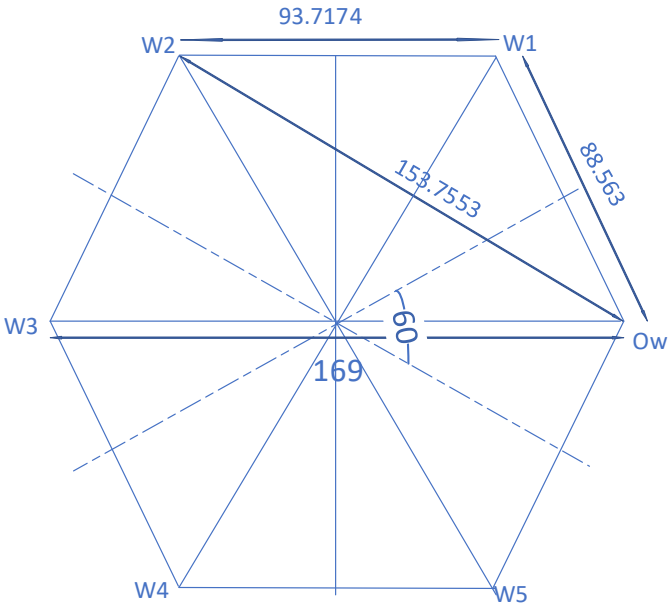

Figure 4.2.2: Inclination of sealing fault at angle 60 at unequal distances from the object well

4.2.3 Procedure of constructing irregular pentagon

1. Construct a regular Heptagon
2. Join two points on the heptagon say in this case, point Ow to W4
3. Do likewise for point W2 to W3

$$Pd = -0.5(EI\left(\frac{-r2}{4t_d}\right) + EI\left(\frac{D1^2}{4t_d}\right) + EI\left(\frac{D2^2}{4t_d}\right) + EI\left(\frac{D3^2}{4t_d}\right) + EI\left(\frac{D4^2}{4t_d}\right)) \quad (22)$$

$$P'_d = 0.5(\exp\left(\frac{-r2}{4t_d}\right) + \exp\left(\frac{D1^2}{4t_d}\right) + \exp\left(\frac{D2^2}{4t_d}\right) + \exp\left(\frac{D3^2}{4t_d}\right) + \exp\left(\frac{D4^2}{4t_d}\right)) \quad (23)$$

Applying our Pd and P'd formula gives us a result similar to that of a regular pentagon yielding number of images to be 3.99

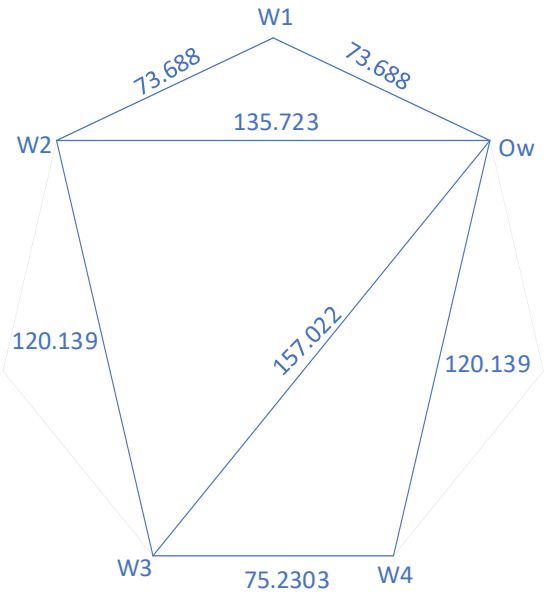

Figure 4.2.3: Inclination of sealing fault at angle 72 at unequal distances from the object well

4.2.4 Procedure to construct a Quadrilateral for unequal side.

1. Simply draw a rectangle

$$Pd = -0.5(EI\ (\frac{-r2}{4t_d}) + EI\ (\frac{D1^2}{4t_d}) + EI\ (\frac{D2^2}{4t_d}) + EI\ (\frac{D3^2}{4t_d})) \quad (24)$$

$$P'_d = 0.5(\exp\ (\frac{-r2}{4t_d}) + \exp\ (\frac{D1^2}{4t_d}) + \exp\ (\frac{D2^2}{4t_d}) + \exp\ (\frac{D3^2}{4t_d})) \quad (25)$$

Applying our Pd and P'd formula gives us a result similar to that of a Square yielding number of images to be 2.99

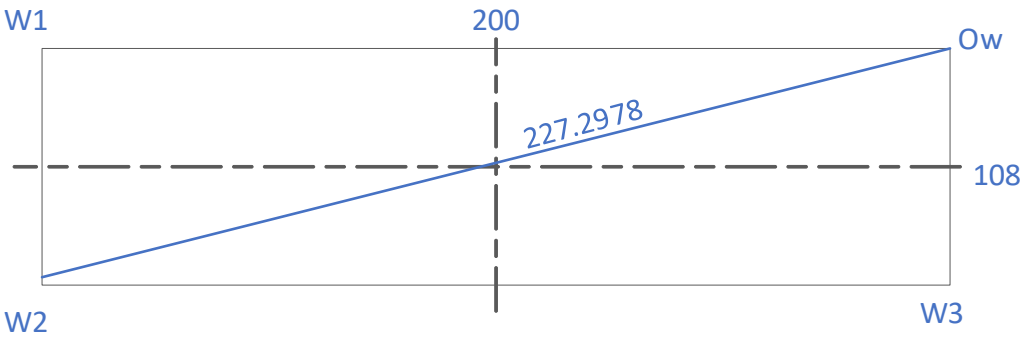

Figure 4.2.4: Inclination of sealing fault at angle 90 at unequal distances from the object well

4.2.5 Procedure to construct an irregular triangle

1. Draw a baseline of any length
2. Extend the end of this line upward (can be perpendicular or at an acute angle to the baseline), also extend the end of the other point
3. Ensure that these two upward lines meet

$$Pd = -0.5(EI\ (\frac{-r2}{4t_d}) + EI\ (\frac{D1^2}{4t_d}) + EI\ (\frac{D2^2}{4t_d})) \quad (26)$$

$$P'_d = 0.5(\exp\ (\frac{-r2}{4t_d}) + \exp\ (\frac{D1^2}{4t_d}) + \exp\ (\frac{D2^2}{4t_d})) \quad (27)$$

Applying our Pd and P'd formula gives us a result similar to that of a regular triangle yielding number of images to be 1.99

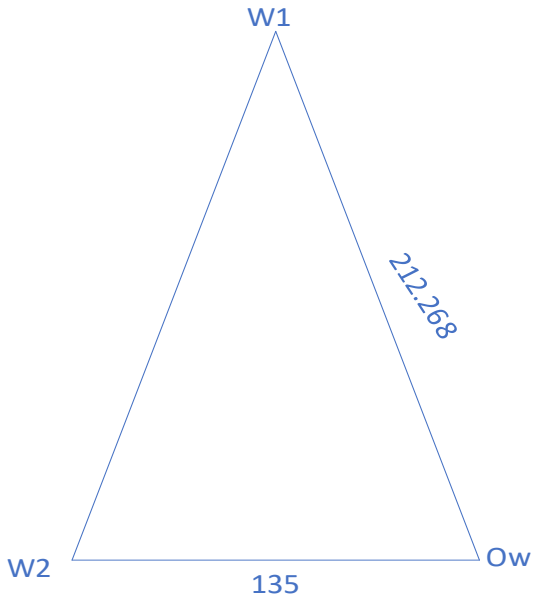

Figure 4.2.5: Inclination of sealing fault at angle 120 at unequal distances from the object well

Table 4.2.1: Table of results for irregular polygons

Θ (angles of inclination)	Number of image wells	Polygons formed
45	6.99	Octagon
60	4.99	Hexagon
72	3.99	Pentagon
90	2.99	Quadrilateral
120	1.99	Triangle

4.2.6 Addition of positive skin to type curves for regular polygons

A generalized formula for the addition of skin

$$Pd = -0.5Ei\left(\frac{-r2}{4td}\right) - 0.5\sum Ei\left(\frac{d}{4^n}\frac{1}{td^n}\right) + s \qquad (28)$$

For example, a quadrilateral would have a formula of d including skin factor.

$$Pd = -0.5(EI\left(\frac{-r2}{4td}\right) + EI\left(\frac{D1^2}{4t_d}\right) + EI\left(\frac{D2^2}{4t_d}\right) + EI\left(\frac{D3^2}{4t_d}\right)) + s \qquad (29)$$

We observe that our pressure derivative are not affected by skin factor although, our dimensionless pressure having a positive skin had similar if not equal wellbore storage for all the polygons obtained. For a skin factor of zero means that there has not occurred any stimulation to enhance the well reservoir performance, we understand that there was a very short middle time region as we confirm a short straight line between the transient and the late time region. Polygons with more sides then to have to have a lager middle time compared to less sided polygons, for instance we can deduce that a hexagon as a more middle time compared to a quadrilateral.

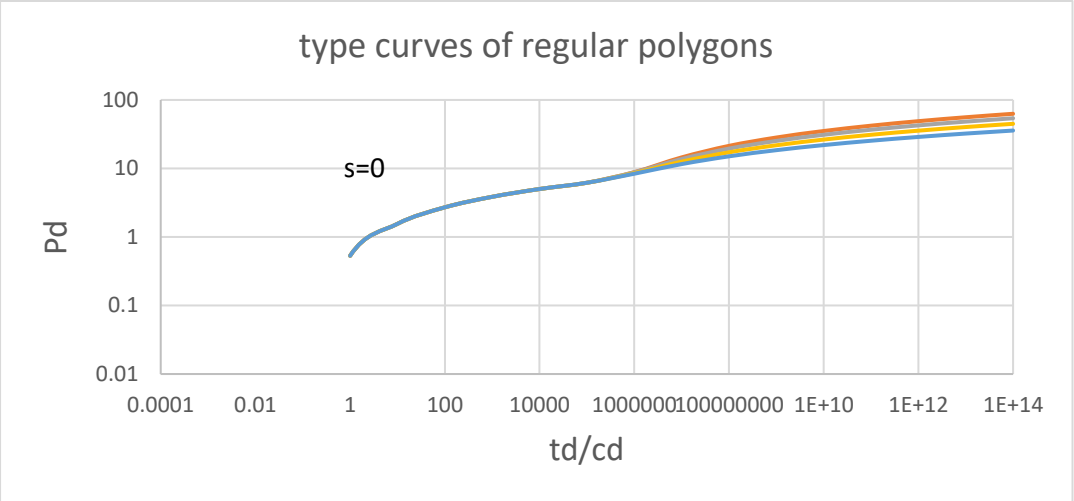

Figure 4.2.6: Type curves of regular polygons with skin factor of zero

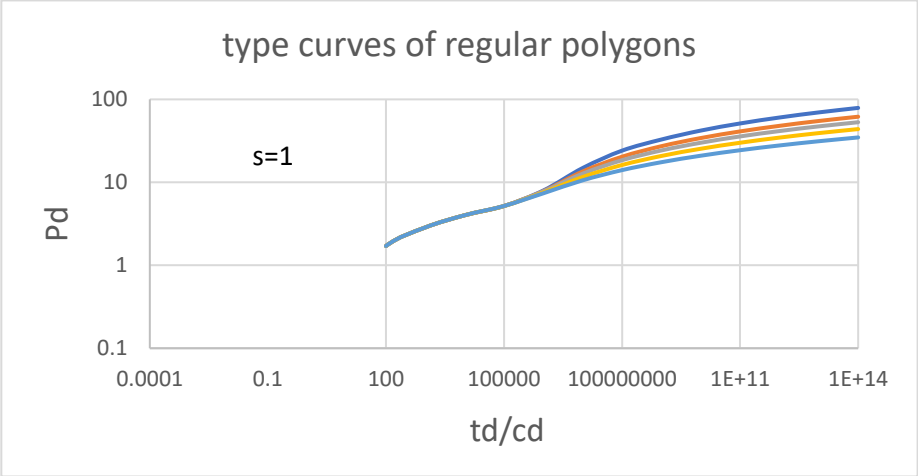

Figure 4.2.7: Type curves of regular polygons with skin factor of one

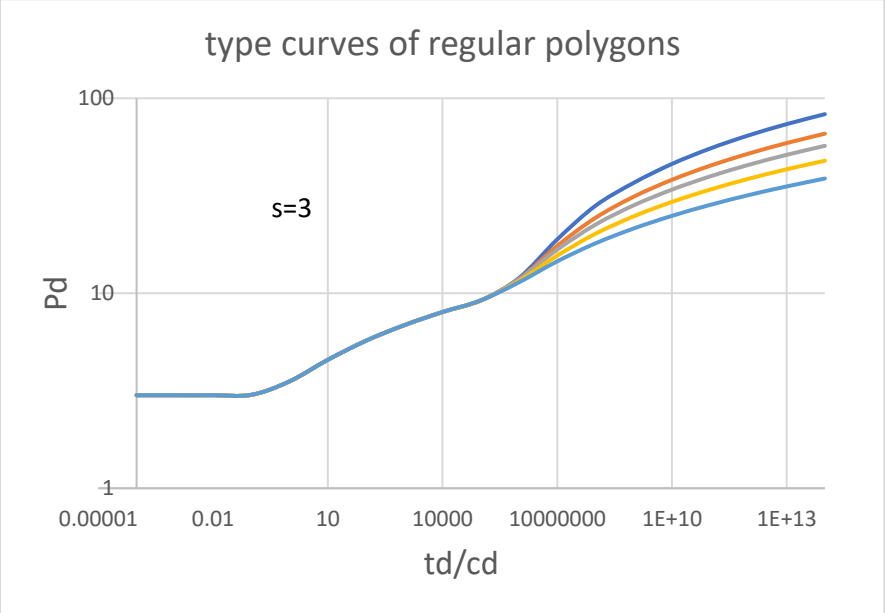

Figure 4.2.8: Type curves of regular polygons with skin factor of three

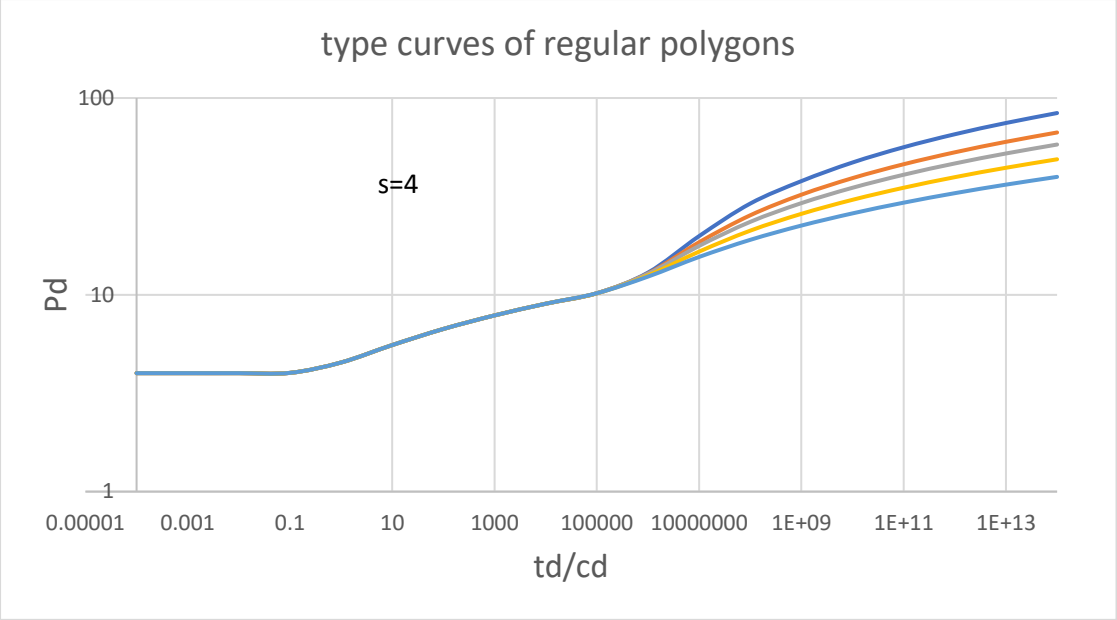

Figure 4.2.9: Type curves of regular polygons of skin factor of four

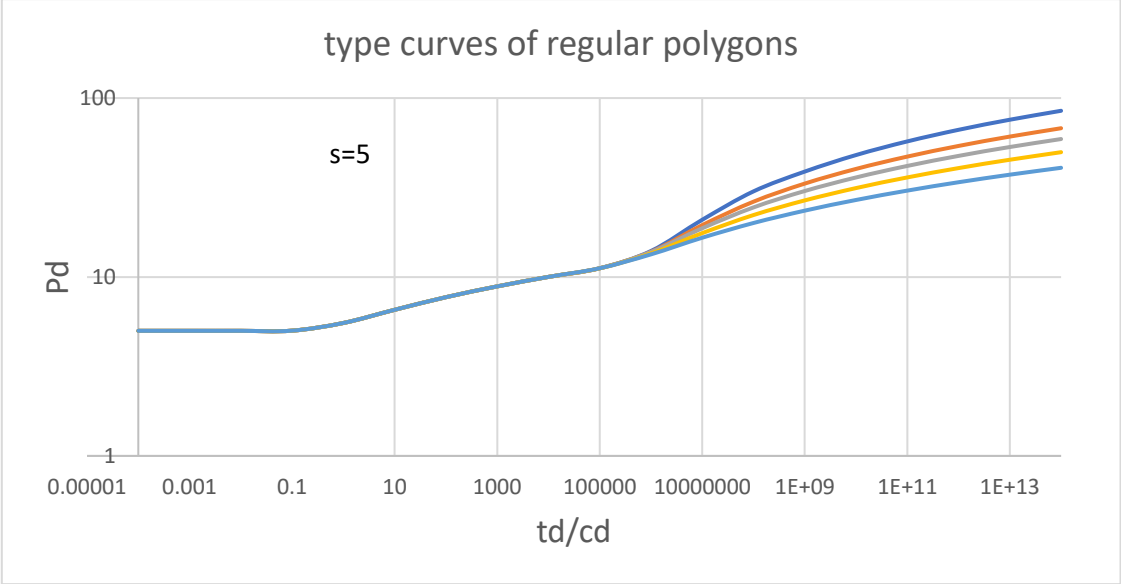

Figure 4.2.10: Type curves of regular polygons of skin factor of five

Skin factor of 1, equal wellbore storage and almost equal middle time region until the skin get larger, do the curves begin to distinctly appear showing a result of increase in skin factor which indicates a damaged well having more larger middle time region before the boundaries are felt.

A more positive skin factor makes the hexagon have more distinct and longer middle-time compared to a quadrilateral or a triangle

4.3 Addition of negative skin to type curves for regular polygons

A negative skin indicates that a well stimulation has occurred which will boost the permeability of the reservoir. From a skin factor of negative one, wellbore storage begins to appear shorter while maintaining the same order of curves from ascending order of a triangle reaching the boundary effects before an octagon. A skin factor of negative two shortens the wellbore storage compared to a factor of -1 meaning that there well enhancement has taken place which the type curves indicate.

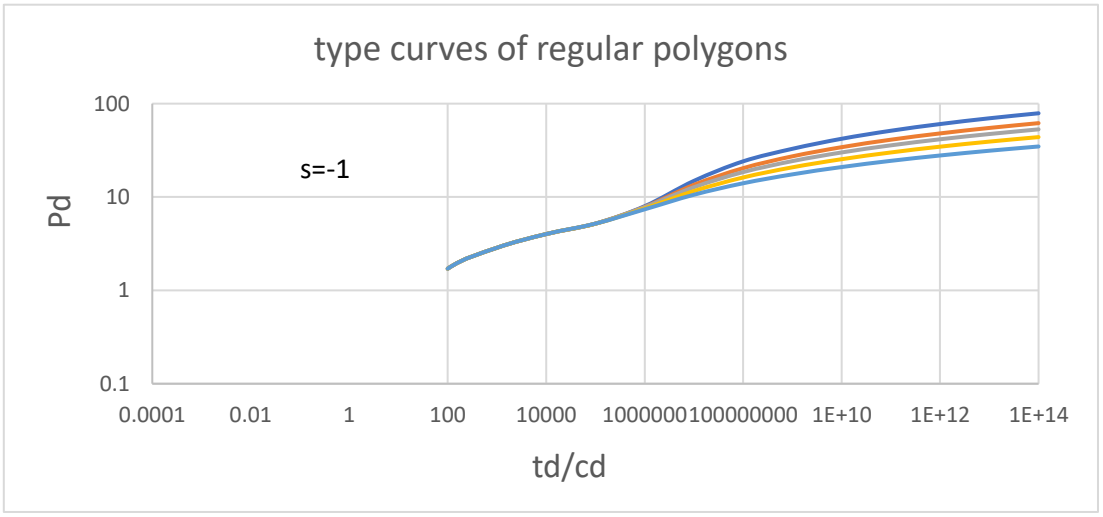

Figure 4.3.1: Type curves of regular polygons of skin factor of negative one

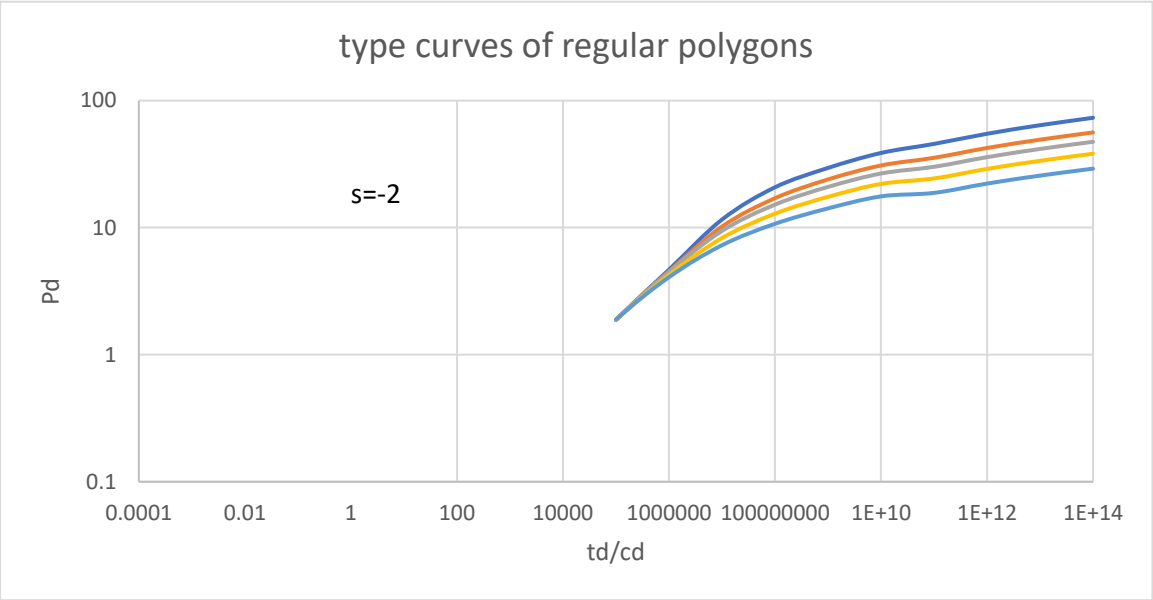

Figure 4.3.2: Type curves of regular polygons of skin factor of negative two

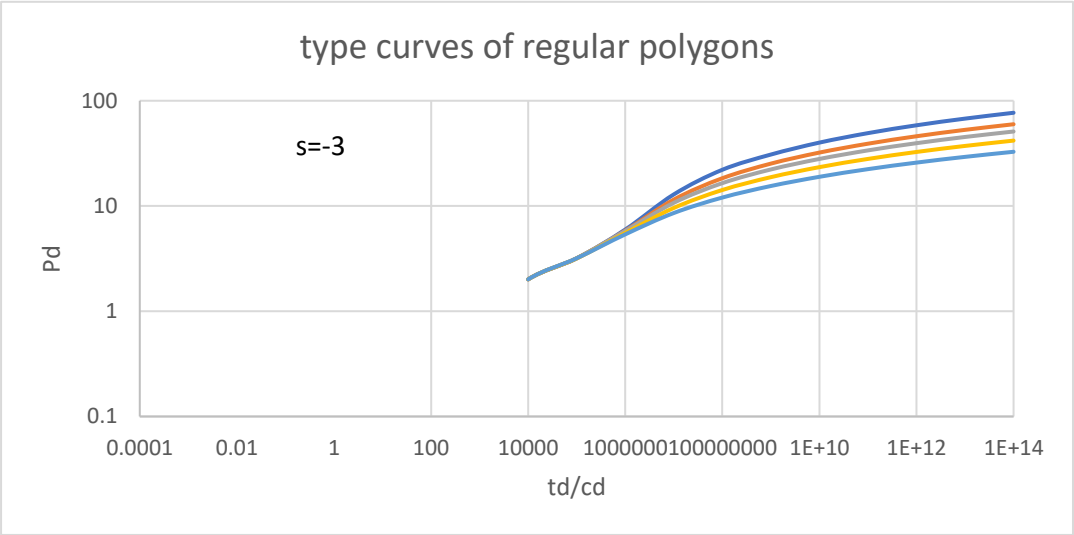

Figure 4.3.3: Type curves of regular polygons of skin factor of negative three

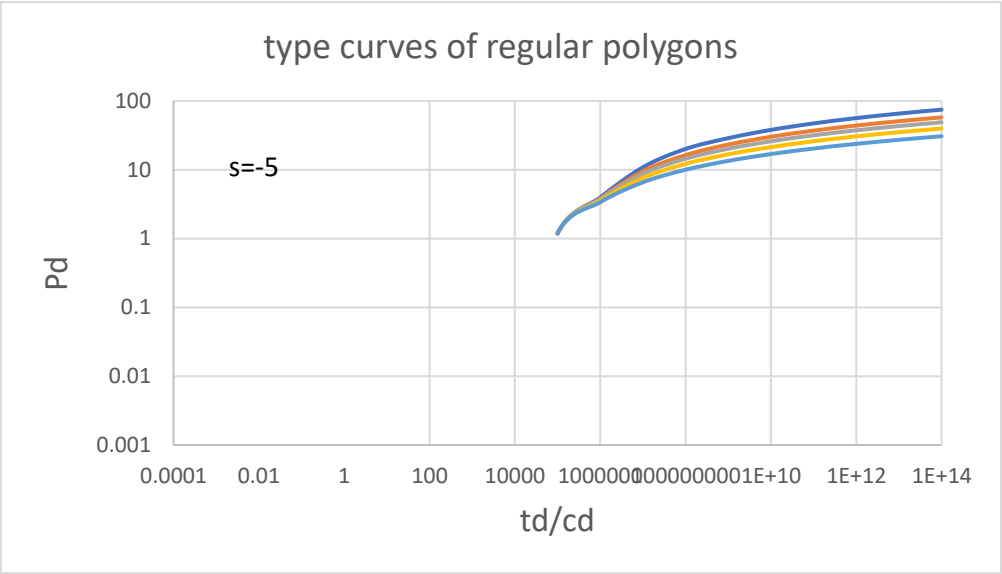

Figure 4.3.4: Type curves of regular polygons of skin factor of negative five

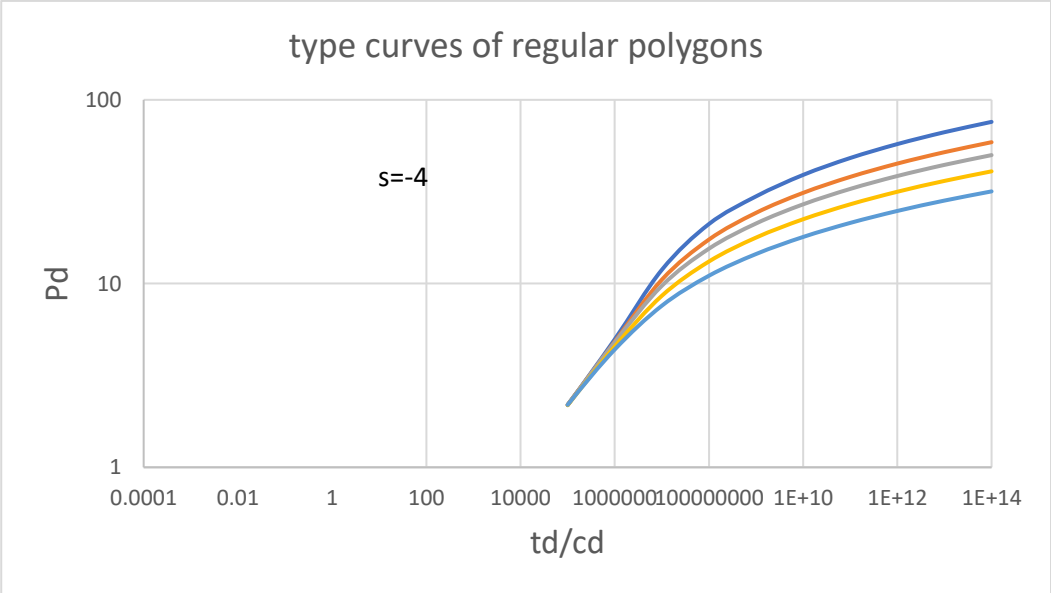

Figure 4.3.5: Type curves of regular polygons of skin factor of negative four

4.4 Addition of positive skin to type curves for irregular polygons

Zero skin factor shows that there has neither enhancement or damage occurred in the wellbore and so a short wellbore storage compared to the regular polygon of same skin factor, meaning an irregular polygon would perform better in terms of enhancement. A longer wellbore storage exists for a more positive skin factor, the curves also appear to be distinctive as the skin factor increases for the octagon having relatively long middle time region in the order of polygons down to the triangle.

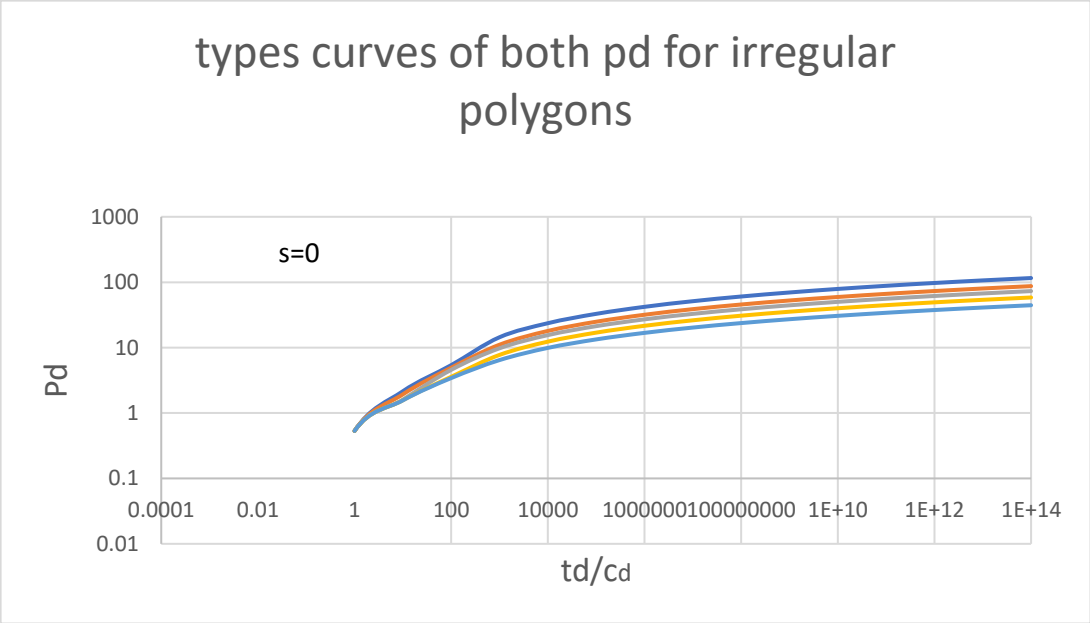

Figure 4.4.1: Type curves of irregular polygons of skin factor of zero

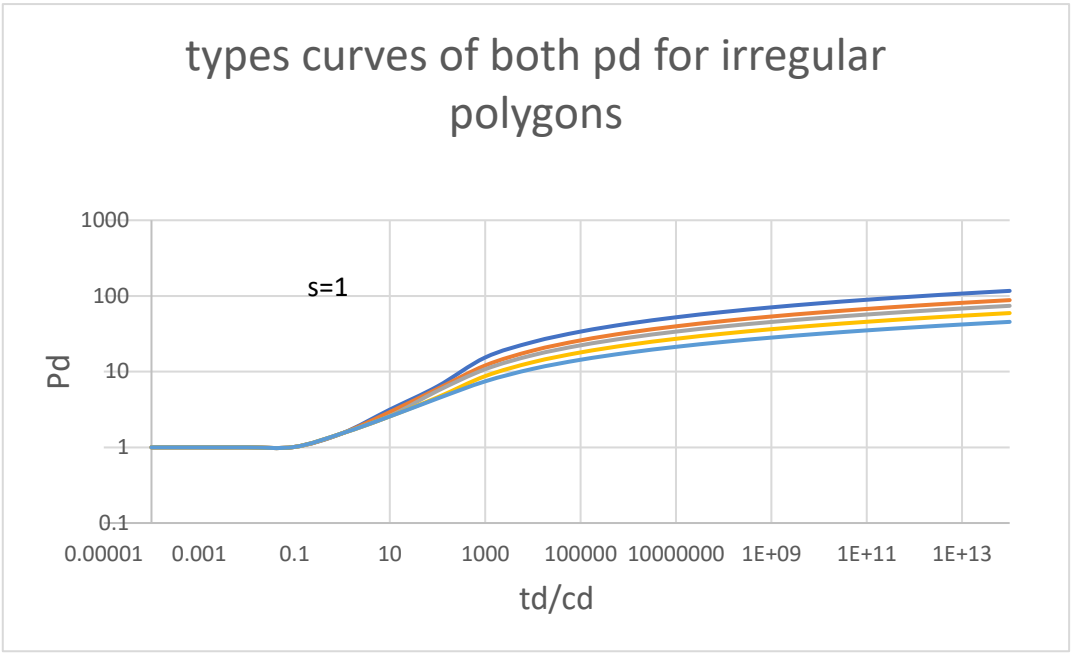

Figure 4.4.2: Type curves of irregular polygons of skin factor of one

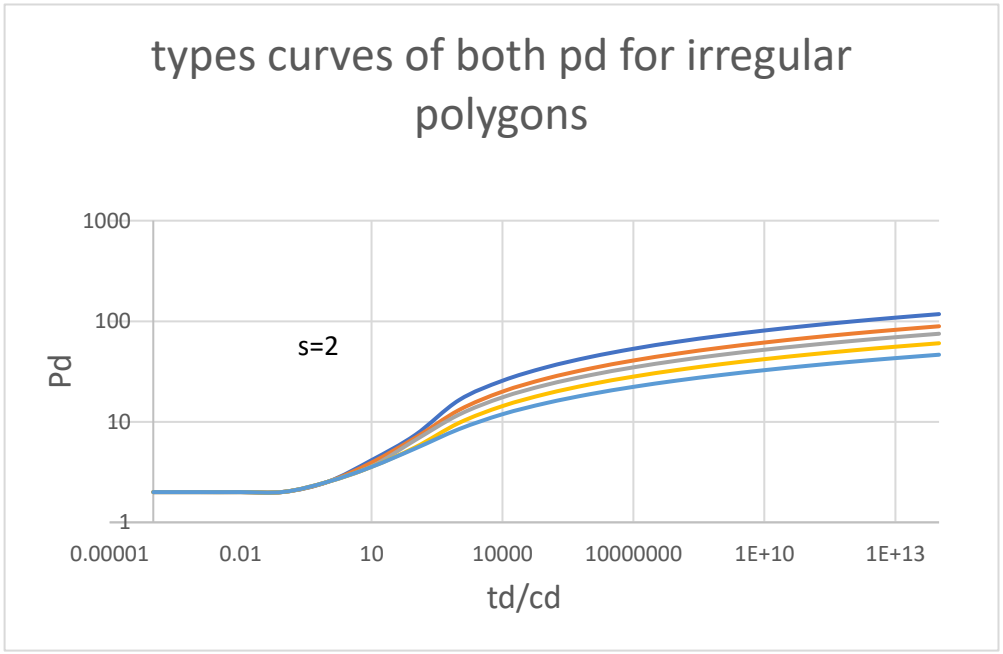

Figure 4.4.3: Type curves of irregular polygons of skin factor of two

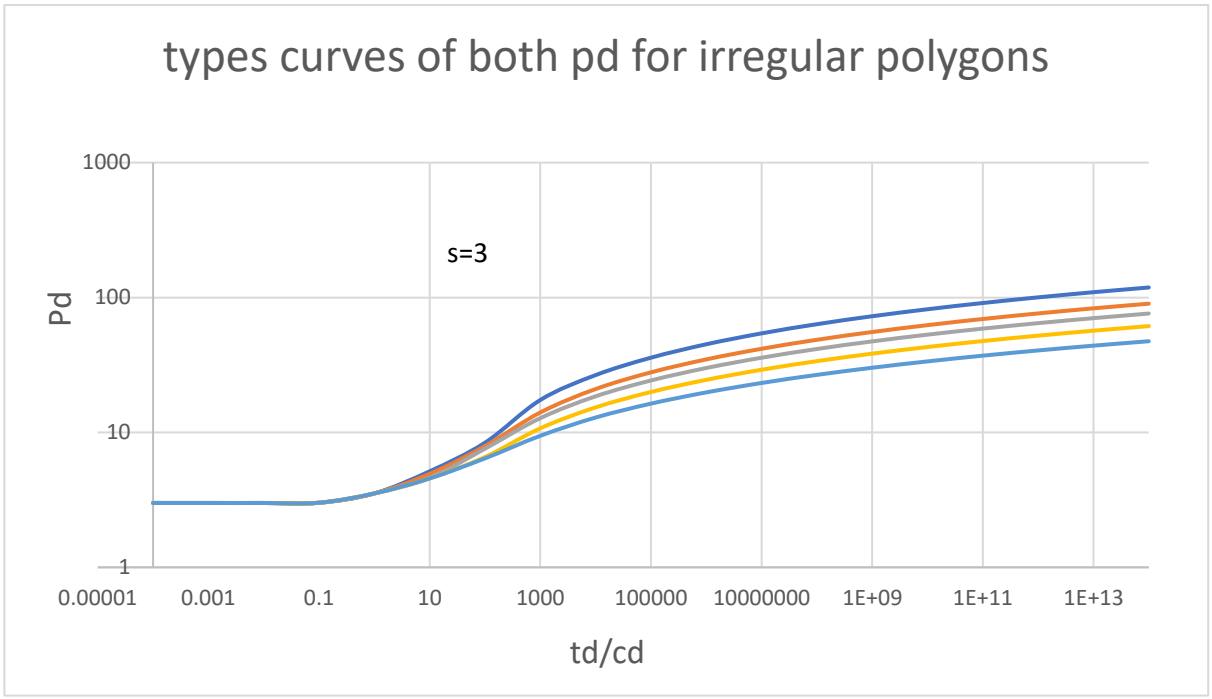

Figure 4.4.4: Type curves of regular polygons of skin factor of three

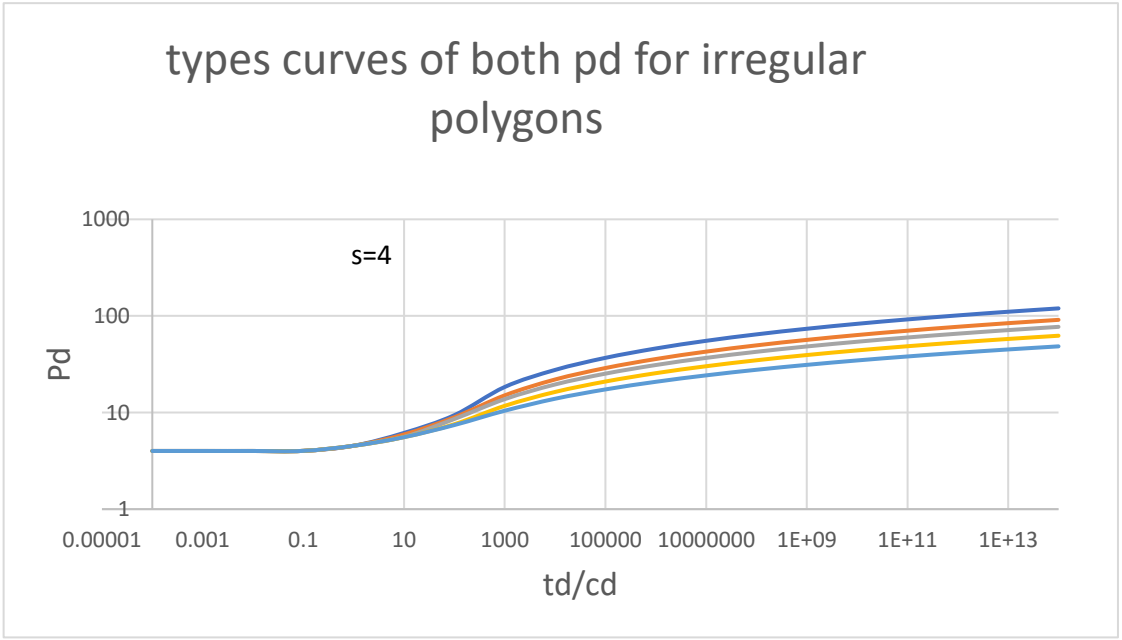

Figure 4.4.5: Type curves of irregular polygons of skin factor of four

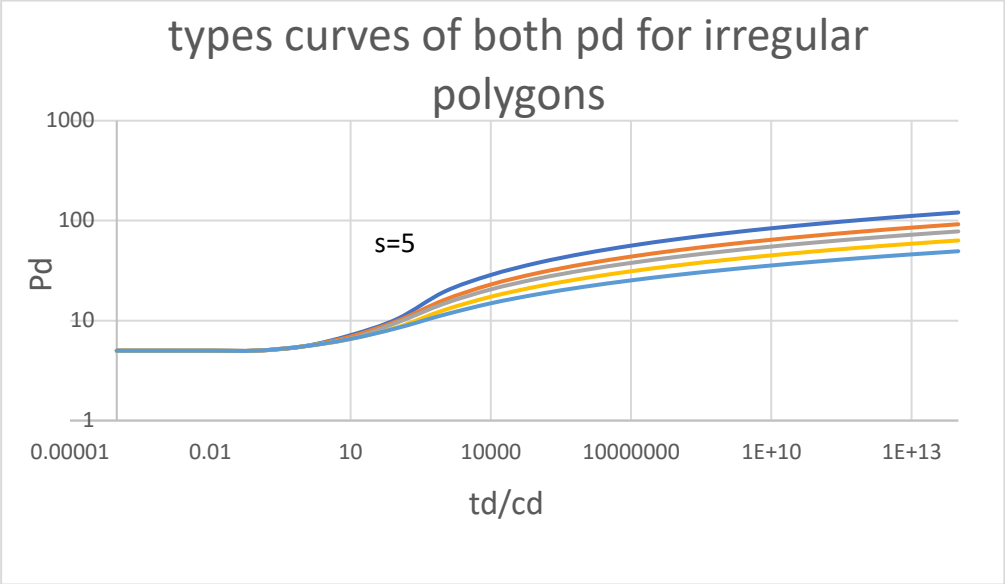

Figure 4.4.6: Type curves of irregular polygons of skin factor of five

4.5 Addition of negative skin to type curves for irregular polygon

Negative skin of an irregular polygons has a very short wellbore storage. A skin factor of -5 gave has the octagon showing a longer middle-time region than all other polygons, skin of -4 has an octagon, hexagon and a quadrilateral having middle time regions. Skin factor of -3 has all the polygons fell the boundary of the reservoir at relatively the same time. The middle time appears for the octagon alone and then for the s=-1, the middle time region of all the polygons shows at almost the same time.

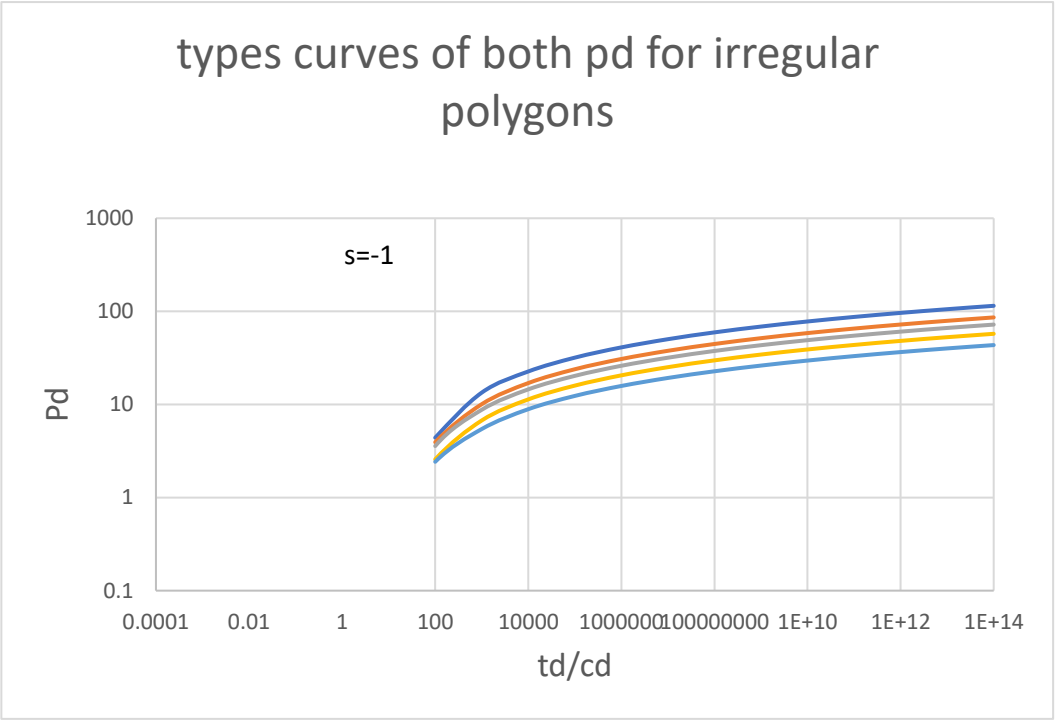

Figure 4.5.1: Type curves of irregular polygons of skin factor of negative one

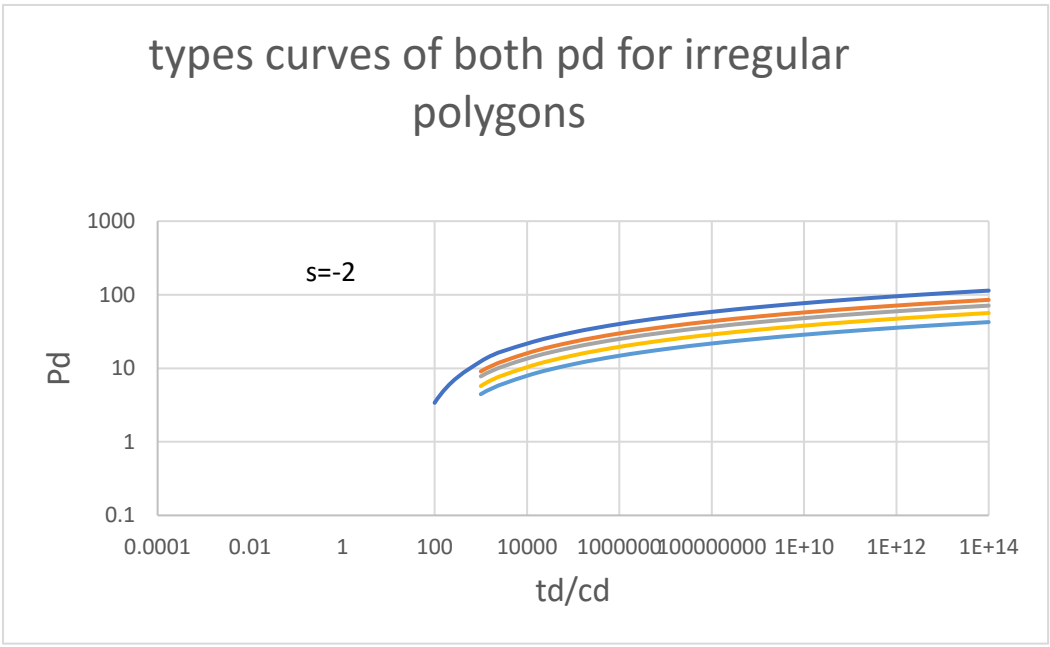

Figure 4.5.2: Type curves of irregular polygons of skin factor of negative two

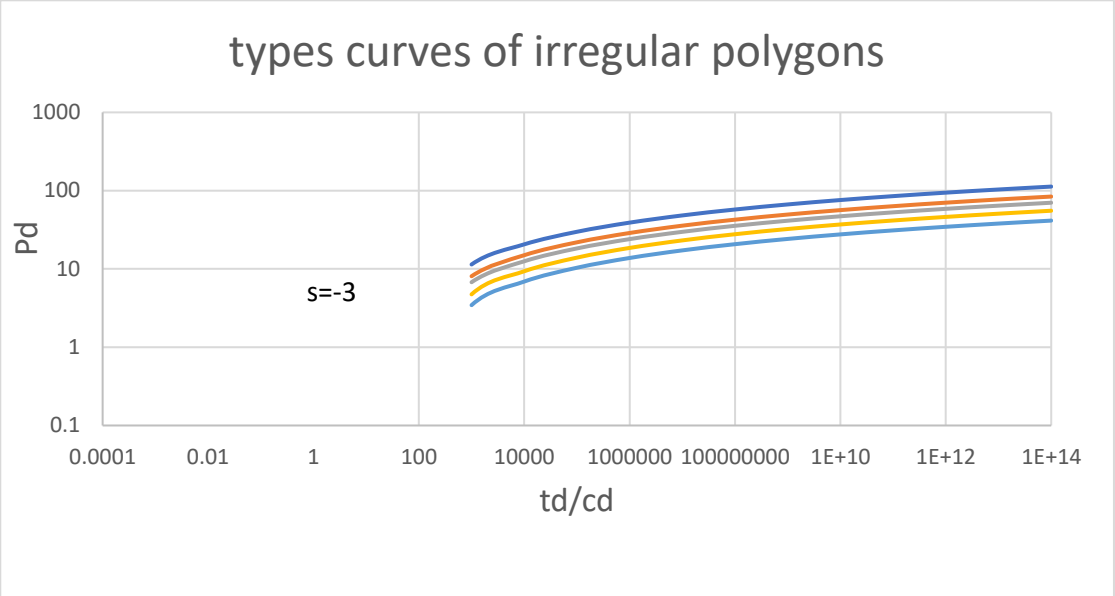

Figure 4.5.3: Type curves of irregular polygons of skin factor of negative three

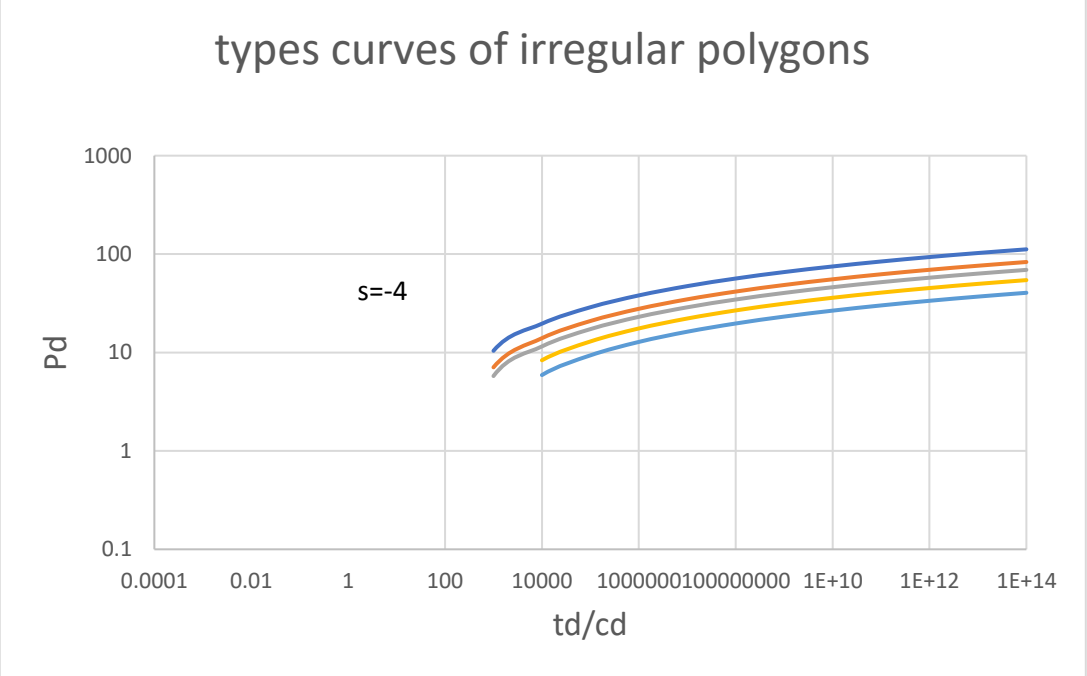

Figure 4.5.4: Type curves of irregular polygons of skin factor of negative four

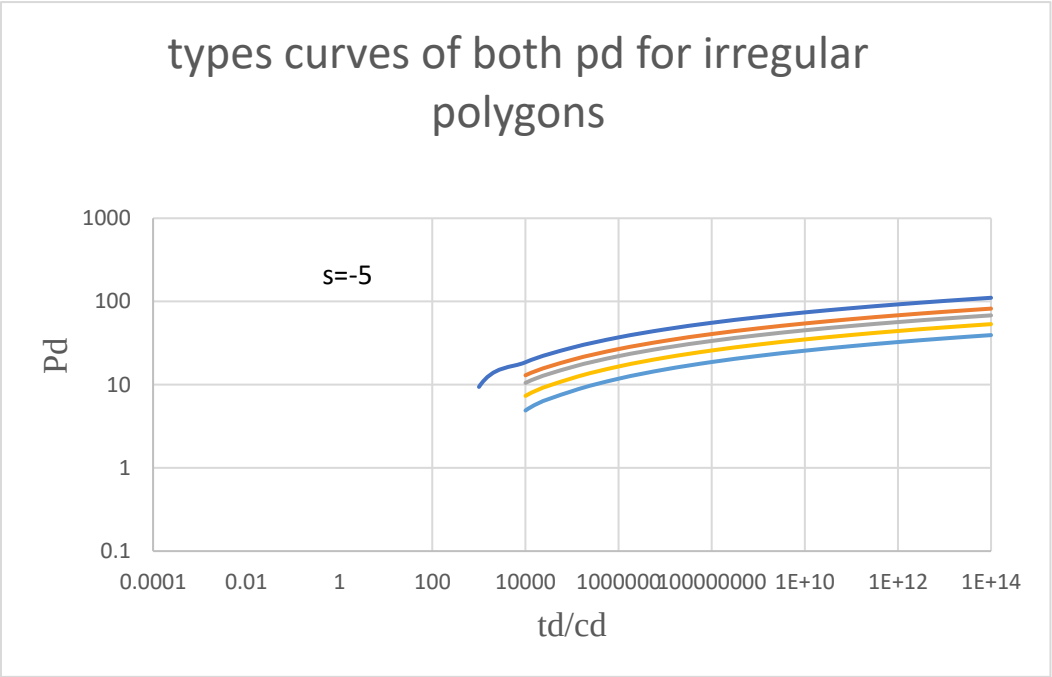

Figure 4.5.5: Type curves of regular polygons of skin factor of negative five

4.6 Addition of wellbore storage to type curves both regular and irregular polygons.

A generalized model for calculating Pd including our wellbore storage is

$$Pd = -0.5Ei\left(\frac{-r2}{\frac{4t_d}{c_d}}\right) + s - 0.5\sum Ei\left(\frac{d}{4^n}\frac{1}{td^n}\right) + s \qquad (30)$$

For example, a quadrilateral which has 90 degrees inclination as a pd formula

$$Pd = -0.5\left(EI\left(\frac{-r2}{\frac{4t_d}{c_d}}\right) + EI\left(\frac{D_1{}^2}{4t_d}\right) + EI\left(\frac{D_2{}^2}{4t_d}\right) + EI\left(\frac{D_3{}^2}{4t_d}\right)\right) + s \qquad (31)$$

Wellbore storage for a skin value of -1 and a cd of 10^3, have octagon, hexagon and pentagon curves of longer middle time than the other curves, explaining the inverse relationship cd and pd. Wellbore storage for a skin value of -1 and a cd of 10^4,10^5 have results similar to cd=10^3

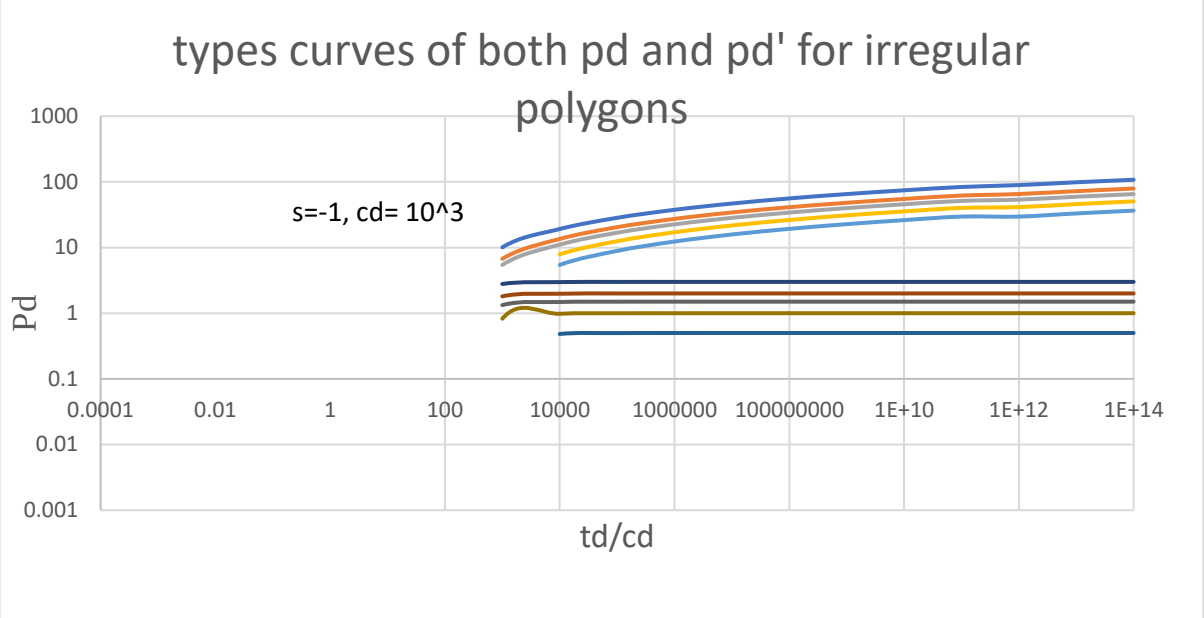

Figure 4.6.1: Type curves of irregular polygons of skin factor of negative one and Cd 10^3

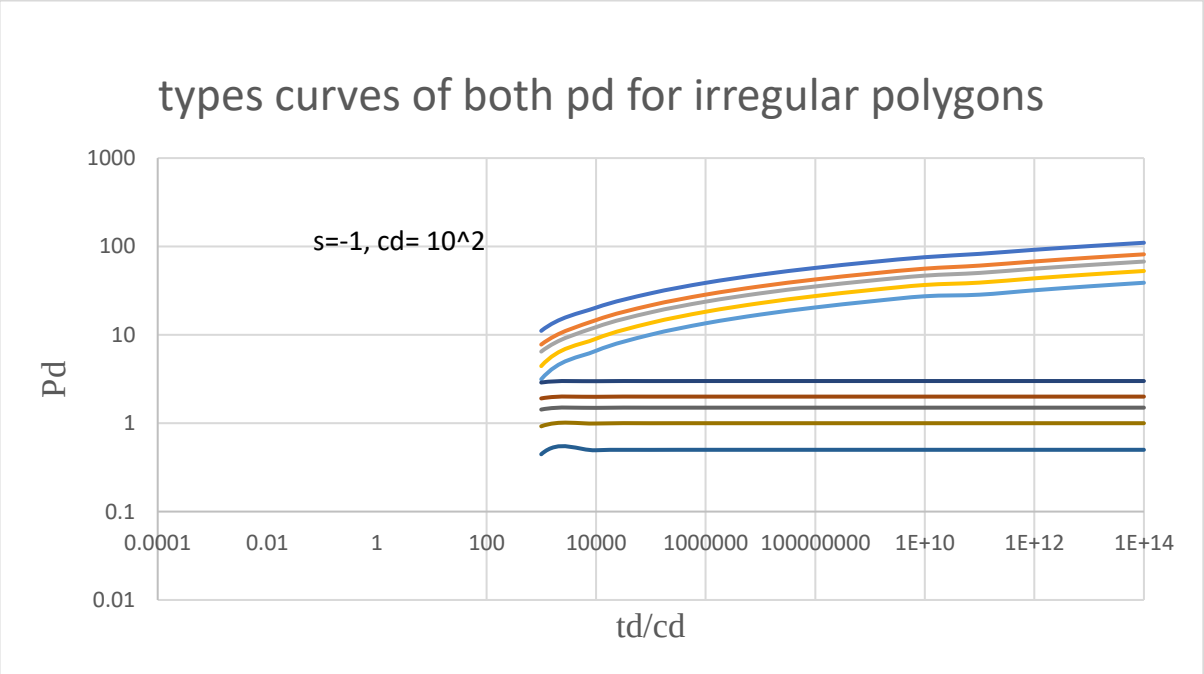

Figure 4.6.2: Type curves of irregular polygons of skin factor of negative one and Cd 10^2

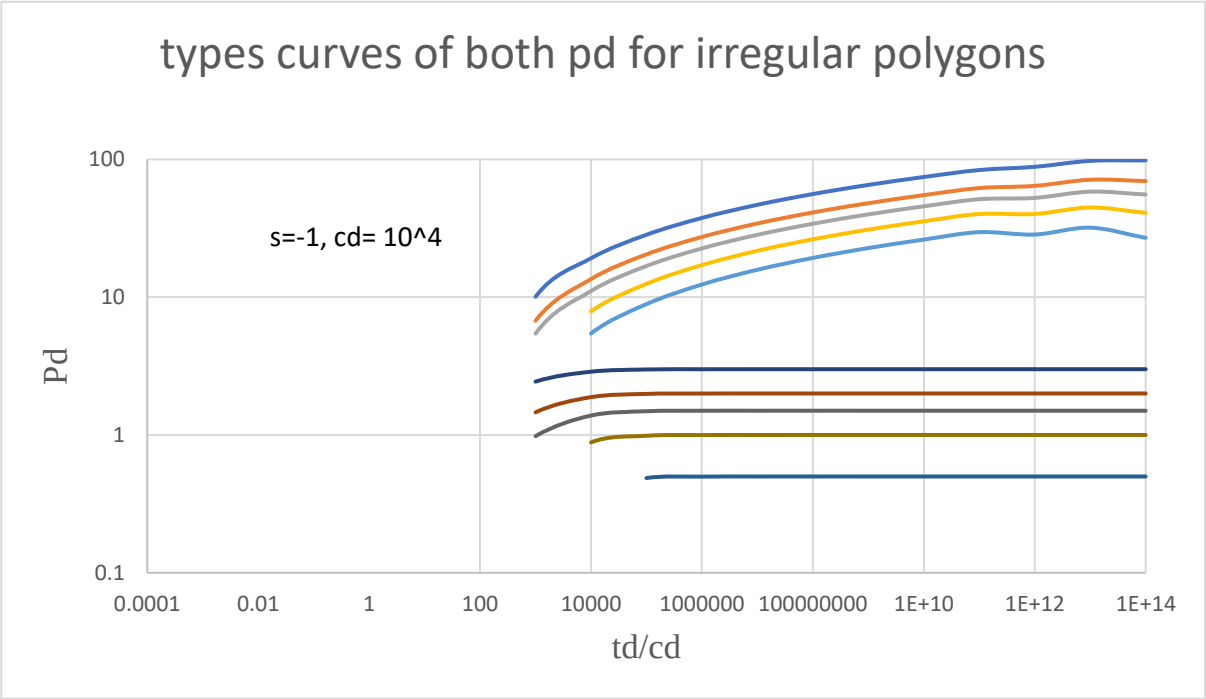

Figure 4.6.3: Type curves of irregular polygons of skin factor of negative one and 10^4

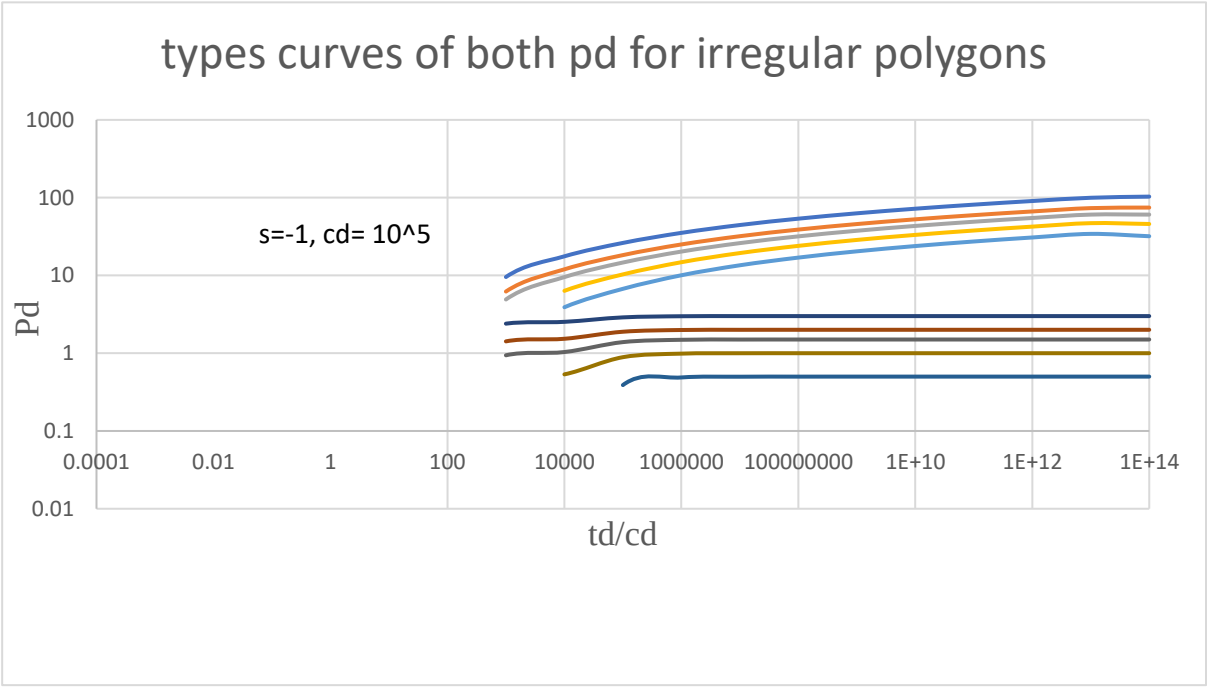

Figure 4.6.4: Type curves of irregular polygons of skin factor of negative one and 10^5

CHAPTER FIVE

5.1 Conclusion

1. Well images of unequal distances between two intersecting faults form irregular polygons which can be difficult to construct since their point of convergence can be uncertain considering the angles of inclination.
2. Relative percentage error of the result for the number of image wells is approximately 0.02 percent
3. Wells are better placed between faults of higher angles of inclination as they produce less image wells, it therefore means that a well polygon of a triangle would take a longer time before the boundaries are felt compared to an Octagon well polygon.
4. In the generation of the curves, two slopes were gotten in which one of them corresponded to the steady-state flow regime until dimensionless time 100000, we then see a transition where the slope reflects our 'n', number of images to indicate that the boundaries are now been felt.
5. Dimensionless pressure gradient is observed to be $1.1513(n+1)$ per cycle.
6. Dimensionless pressure derivative is observed to be $0.5(n+1)$

5.2 Recommendation

1. Software application such as Microsoft Visio can aid in the construction of both regular and irregular polygons.
2. Microsoft excel is an excellent application software that enables the numerical computation analysis.

REFERENCES

Adewole, E.S. (2021): "Signatures of a Horizontal Well Completed Near a Sealing Boundary", Lecture presented in the Lecture Series of Society of Petroleum Engineers, Lagos Section 61 Lecture Series, Virtual, March 31.

Aiankho V Ogbamikhumi,. Adewole E.S. (2021): "Characteristics of Dimensionless Pressure Gradients and Derivatives of Horizontal and Vertical Wells Completed within Inclined Sealing Faults" paper 207179 presented at the Society of Petroleum Engineers Nigeria Annual International Conference and Exhibition, Lagos, Nigeria, 2–4, August 2021.

Bourdarot, G. (1998). *Well Testing: Interpretation Methods*. EDITIONS TECHNIP.

Britton, P.R. and Grader, A.S. (1988): "The Effects of Size, Shape, and Orientation of an Impermeable Region on Transient Pressure Testing", SPE Formation Evaluation, 3, 595-606.

Davis, E.G. and Hawkins, M.F. (1963): "Linear Fluid-Barrier Detection by Well Pressure Measurements", Journal of Petroleum Technology, 15, 1077-1081.

Earlougher, R.C. Jr. (1977): Advances in Well Test Analysis, Monograph Series, SPE, Dallas.

Gerard, M. and Horne, R.N. (1985): "Effects of external boundaries on the recognition of reservoir pinch out boundaries by pressure transient analysis", Soc. Pet. Eng. June, pp. 427-436.

Johnson Orene Johnson, Adewole E.S. (2021): "Flow Behaviour of a Horizontal Well Completed within Sealing Faults Inclined at Right Angle" paper 207186 presented at the Society of Petroleum Engineers Nigeria Annual International Conference and Exhibition, Lagos, Nigeria, 2–4, August.

Martinez, S. and Cinco-Ley. H., (1985): "Detection of linear impermeable barriers by transient pressure analysis" paper to SPE, Richardson, Texas.

Matthews, C.S and Russell, D.G., (1967): Pressure buildup and flow tests in wells. SPE of AIME, Dallas, Texas.

Michael G Ojah, Adewole E.S. (2021): "Pressure and Pressure Derivatives of a Vertical Well Located Within Two Inclined Faults: Case Study of Basic Angles and Unequal Well Distances from Faults", paper 207138 presented at the Society of Petroleum Engineers Nigeria Annual International Conference and Exhibition, Lagos, Nigeria, 2–4, August.

Overpeck, A.C and Holden, W.R., (1970): "Well imaging and fault detection in anisotropic reservoirs", J. Pet. Tech., Oct., pp. 1317-1325; Trans., AIME, 249.

Oduh, P. O, Ezekiel Ayobami, Okoh Emmanuel, Collins Onah, Michael G Ojah and Adewole E.S. (2021): "Numerical Method of Estimating Distance between Wells" paper 207159 presented at the Society of Petroleum Engineers Nigeria Annual International Conference and Exhibition, Lagos, Nigeria, 2–4, August.

Prasad, Raj K., (1975): "Pressure transient analysis in the presence of two intersecting boundaries", J. Pet. Tech., Jan., 89-96; Trans., AIME, 259.

Tiab, D. and Kumar, A. (1980): "Detection and Location of Two Parallel Sealing Faults around a Well", Journal of Petroleum Technology, 20, 1701-1708.